



Journal of The Ferrata Storti Foundation

Role of Epstein Barr virus in transformation of follicular lymphoma to diffuse large B-cell lymphoma: a case report and review of the literature

by Massimo Granai, Maria Raffaella Ambrosio, Ayse Akarca, Lucia Mundo, Federica Vergoni, Raffaella Santi, Virginia Mancini, Gioia Di Stefano, Teresa Amato, Cristiana Bellan, Benedetta Puccini, Ester Sorrentino, Kikkeri N. Naresh, Lorenzo Leoncini, Teresa Marafioti, and Stefano Lazzi

Haematologica 2019 [Epub ahead of print]

Citation: Massimo Granai, Maria Raffaella Ambrosio, Ayse Akarca, Lucia Mundo, Federica Vergoni, Raffaella Santi, Virginia Mancini, Gioia Di Stefano, Teresa Amato, Cristiana Bellan, Benedetta Puccini, Ester Sorrentino, Kikkeri N. Naresh, Lorenzo Leoncini, Teresa Marafioti, and Stefano Lazzi.

Role of Epstein Barr virus in transformation of follicular lymphoma to diffuse large B-cell lymphoma: a case report and review of the literature.

Haematologica. 2019; 104:xxx

doi:10.3324/haematol.2018.215053

Publisher's Disclaimer.

E-publishing ahead of print is increasingly important for the rapid dissemination of science. Haematologica is, therefore, E-publishing PDF files of an early version of manuscripts that have completed a regular peer review and have been accepted for publication. E-publishing of this PDF file has been approved by the authors. After having E-published Ahead of Print, manuscripts will then undergo technical and English editing, typesetting, proof correction and be presented for the authors' final approval; the final version of the manuscript will then appear in print on a regular issue of the journal. All legal disclaimers that apply to the journal also pertain to this production process.

Role of Epstein Barr virus in transformation of follicular lymphoma to diffuse large B-cell lymphoma: a case report and review of the literature.

Massimo Granai ¹, Maria Raffaella Ambrosio ¹, Ayse Akarca ², Lucia Mundo ¹, Federica Vergoni ³, Raffaella Santi ³, Virginia Mancini ¹, Gioia di Stefano ³, Teresa Amato¹, Cristiana Bellan ¹, Benedetta Puccini ³, Ester Sorrentino ¹, Kikkeri N. Naresh ⁴, Lorenzo Leoncini ¹, Teresa Marafioti ², Stefano Lazzi ¹.

¹Section of Pathology, Department of Medical Biotechnology, University of Siena, Siena, Italy

²Department of Histopathology, University College London Hospital, London, UK

³Section of Pathology, University of Florence, Florence, Italy

⁴Hammersmith Hospital & Imperial College, London UK

Correspondence: Lorenzo Leoncini, lorenzo.leoncini@dbm.unisi.it.

The Epstein-Barr virus (EBV) is the most common human virus, implicated in the pathogenesis of several human tumors, particularly B-cells lymphoma¹. EBV-induced lymphoproliferative disorders (EBV-LPDs) are the result of the outgrowth of EBV-infected B-cells, that would normally controlled by an effective EBV-specific cytotoxic T-cell response^{2, 3}. The association between EBV and follicular lymphoma (FL) is not well recognized and only 10 cases have been previously described^{4,5,6,7}. Nine of them showed EBER-positivity in >75% of tumour cells and one case in ~5–10%. EBV-positivity was associated with grade 3 FL (9/10), CD30 expression and rapid progression of disease⁶. However, it is still unclear whether EBV infection is an early event in the development of FL or a late event that may contribute to the progression of a pre-existing lymphoma. We describe a case of EBV-positive diffuse large B-cell lymphoma (DLBCL) evolved from a previous FL.

In April 2011, a 73-year old woman presented with systemic lymphadenopathy and history of weakness. A right inguinal lymph node was removed. Histological examination showed complete effacement of the nodal architecture by closely packed follicles, with attenuated mantle zones, loss of polarity and absence of tingible body macrophages. The tumor cells expressed CD20, CD10, BCL-2, BCL-6 and focally CD30. The proliferation index (Ki-67) was about 20%. FISH by Break-Apart probe (BAP) identified the typical *IGH-BCL2* translocation. Due to the involvement of multiple extranodal sites, a diagnosis of FL, grade 2, stage IVA (Ann Arbor system) was made. The patient was treated with four cycles of rituximab *plus* fludarabine, mitoxantrone, and dexamethasone, followed by maintenance therapy (rituximab). The treatment was discontinued in 2013 for the disease's progression. Biopsy of a right axillary lymph node was performed, confirming the previous diagnosis with increased proliferative index (40%). The patient was placed in a "watch and wait" program. In March 2016, a follow-up computerized tomography (CT) scan revealed a mediastinal and abdominal lymph nodes enlargement and laboratory tests showed serum lactate dehydrogenase (LDH) increase. The patient started the rituximab *plus* cyclophosphamide, vincristine and prednisolone protocol which was interrupted in March 2017, due to pulmonary intolerance. A new regimen with rituximab and fludarabine *per os* was started. In November 2017, the patient was hospitalized for recurrent not infectious fever and a left inguinal-crural lymph node biopsy was performed. Histological examination showed the presence of a diffuse proliferation of large lymphoid cells intermingled with areas of FL grade 2 and areas of necrosis (Figure 1A-C). The neoplastic cells of both component expressed PAX-5, CD10, BCL-2, BCL-6, MUM-1 and CD30. The proliferative index (Ki-67) was 70% in the diffuse areas. BAP-FISH identified *BCL2* translocation in both areas (Figure 1 D-E). LMP-2A and EBV-encoded RNAs (EBER) *in situ* hybridization (ISH) positivity was present in 90% of the neoplastic cells in the diffuse area and

within scattered cells in the follicular area (Figure 1 F-G). A diagnosis of DLBCL transformed from FL was proposed. Due to patient's critical clinical condition and high viral load of cytomegalovirus (CMV) (32,461 copies) and EBV (24,212 copies) in the serum, the patient was treated by rituximab and lenalinomide *plus* valgancyclovir for the CMV infection. To evaluate whether we were dealing with the transformation of the pre-existing FL, a comparative evaluation of the original FL and DLBCL specimens was made in terms of clonality, EBV status and tumour microenvironment (TME). To assess B-cell clonality, *IGH-VDJ* rearrangement was performed in all the specimens according to BIOMED-2 protocol. Specifically, to evaluate whether the EBV-positive population observed in the histologic sections of DLBCL corresponded to the follicular population, we performed a laser capture microdissection (LMC) of the diffuse and follicular areas of the 2017 biopsy (Figure 2 A-B). A peak of 316 base pairs (bp) in length was identified in both (Figure 2 C-D). Then, we checked EBV status also in the 2011 and 2013 FL samples and we found the virus in 5% (2011) and 10% (2013) of neoplastic cells within the follicles (Figure 2 E-F). After LMC, the clonal analysis of the 2011 and 2013 FL samples identified a peak with the same length of the 2017 one (316 bp) (Figure 2 G-H). The corresponding FR1-JH PCR products of all the samples were directly sequenced and a productive *IGHV-D-J* rearrangement (V1-18*01, D3-9*01 and J4*02) with 86.76% homology of germ-line sequence was detected, confirming the clonal relationship (Figure 2 I). Furthermore, in all the biopsies, we detected an identical somatic hypermutation pattern and the same N-glycosylation motif (NTT) in the HCDR3 region (Figure 2 J). Since the oncogenic role of EBV in leading the transformation of FL to a high-grade form is still controversial, a complete genetic assessment of the virus latency by RT-qPCR and immunohistochemistry was performed. The expression of EBNA-1 and the negativity for LMP-1 and EBNA-2 in the FL specimen suggested a type I latency. In the DLBCL sample, we detected a non-canonical latency pattern of neoplastic cells characterized by the expression of LMP-2A along with some genes/proteins involved in the lytic cycle [*BMRF1/Ea-D*, *BHRF1/ Ea-R/p17* and *BZLF1/Zebra* (Figure 1 G inset)]. Finally, we studied the TME of FL and DLBCL specimens to identify a possible alteration of the EBV-host balance responsible of the evolution. In the FL sample, the neoplastic follicles showed a low number of regulatory T-cells (CD4/FOXP3 double positive and CD25/FOXP3/CTLA-4 triple positive) (Figure 3 A, B) and triple positive CD8/PD1/Granzyme B T-cells (Figure 3 C). The scenario was different in the transformed DLBCL biopsy showing increased regulatory and triple-positive CD8/PD1/Granzyme B T-cells (Figure 3 E, F and G). The latter were concentrated at the periphery of the necrotic areas; the centre of the necrotic area showed a significant CD8 single-positive T-cells increase. In the FL sample numerous CD163/c-MAF double positive macrophages (M2 macrophages) were found in the interfollicular

areas accompanied by occasional CD163/PD-L1 double positive cells (Figure 3 D). In DLBCL, the M2 macrophages increased; the great majority expressed PD-L1 (Figure 3 H). PD-L1 expression was also demonstrated in scattered neoplastic cells (Figure 3 H inset).

Due to the clinical worsening, the patient died in June 2018.

The process of transformation has some confounding factors: impact of chemotherapy on immune microenvironment; role of immune system; proliferative advantage provided by EBV; impact of EBV latency program modification and expression of additional EBV products; and natural evolution of FL independent from EBV. Our case favors the hypothesis that EBV was the trigger responsible for the transformation of FL in DLBCL, under permissive immunologic conditions. Indeed, the evidence of EBV lytic cycle reactivation in the DLBCL sample and the expression of a non-canonical latency program, as demonstrated by RT-qPCR and IHC, may shed light on the effective role of the virus in the transformation of the disease and in the maintenance of an immunosuppressive niche. Conventionally, EBV-driven lymphomagenesis is thought to primarily involve latent cycle, but there is increasing evidence that lytic gene products contribute to the development and maintenance of malignancies through the induction of growth factors, oncogenic cytokine production such as interleukin 10 (IL-10), transforming growth factor (TGF β)^{9,10,11} and the evasion of inflammatory response by attenuation of IFN γ ¹². Furthermore, we were able to demonstrate the clonal relationship between the diffuse areas and follicular components in all the three biopsies and direct sequencing of the FR1-JH PCR products showed an identical IGHV-D-J rearrangement. These findings were also consolidated by the identification of an identical somatic hypermutation pattern and the same NTTs which are characteristic of FL and uncommon in other B-cell malignancies⁸.

The role of the virus in the transformation is further supported by the changes induced in TME. In fact, a valuable CD4/PD-1 T-cells population control the response against the virus in the follicular components². Following the chemotherapy, the balance between EBV and host immune system might have been disrupted leading to an unchecked EBV activation resulting in a non-canonical latency of the virus in the DLBCL sample and changes in the inflammatory microenvironment⁹. In fact, in the diffuse areas, we found an increased number of T-regulatory cells and triple-positive CD8/PD1/Granzyme B T-cells as well as the expression of PD-L1 on M2 macrophages and lymphoid cells. The PD-1/PD-L1 pathway is a key check-point in controlling the re-education of the tumour microenvironment¹³, diminishing activation of tumor infiltrating lymphocytes (TILs) and inhibiting phagocytosis and tumour immunity, promoting lymphoma growth¹⁴. This pattern seems to be different from the EBV negative DLBCL in which the number of M2 macrophages

expressing PD-L1 is lower than in our case. (Preliminary results, Prof. Marafioti *et al.*- manuscript in preparation).

Notwithstanding these evidences, the precise role of EBV lytic activity and its ability to reshape the TME remains elusive and further investigation is warranted.

However, our findings expand the spectrum of recognized EBV-associated B-cell lymphomas and raise the question as to whether EBV association should be investigated in cases of FL to establish its relationship to lymphomagenesis or transformation.

REFERENCES

1. Dojcinov SD, Fend F, Quintanilla-Martinez L. EBV-Positive Lymphoproliferations of B- T- and NK-Cell Derivation in Non-Immunocompromised Hosts. *Pathogens*. 2018;7(1):28.
2. Cocco M, Bellan C, Tussiwand R, et al. CD34+ cord blood cell-transplanted Rag2^{-/-} gamma(c)^{-/-} mice as a model for Epstein-Barr virus infection. *Am J Pathol*. 2008;173(5):1369-78.
3. Linke-Serinsöz E, Fend F, Quintanilla-Martinez L. Human immunodeficiency virus (HIV) and Epstein-Barr virus (EBV) related lymphomas, pathology view point. *Semin Diagn Pathol*. 2017;34(4):352-363.
4. Orlandi E, Paulli M, Viglio A et al. Epstein–Barr virus - positive aggressive lymphoma as consequence of immunosuppression after multiple salvage treatments for follicular lymphoma. *Br J Haematol*. 2001;112(2):373-376.
5. Menon MP, Hutchinson L, Garver J, Jaffe ES, Woda BA. Transformation of follicular lymphoma to Epstein-Barr virus-related Hodgkin-like lymphoma. *J Clin Oncol*. 2013;31(5):e53-e56.
6. Mackrides N, Campuzano - Zuluaga G, Maque - Acosta Y, et al. Epstein - Barr virus - positive follicular lymphoma. *Mod Pathol*. 2017;30(4):519-529.
7. Mackrides N, Chapman J, Larson MC, et al. Prevalence, clinical characteristics and prognosis of EBV-positive follicular lymphoma. *Am J Hematol*. 2019;94(2):E62-E64.
8. Zhu D, McCarthy H, Ottensmeier CH, Johnson P, Hamblin TJ, Stevenson FK. Acquisition of potential N-glycosylation sites in the immunoglobulin variable region by somatic mutation is a distinctive feature of follicular lymphoma. *Blood*. 2002;99(7):2562-2568.
9. Cohen M, Vistarop AG, Huaman F, et al. Epstein-Barr virus lytic cycle involvement in diffuse large B cell lymphoma. *Hematol Oncol*. 2018;36(1):98-103.

10. Ma SD, Hegde S, Young KH, et al. A new model of Epstein-Barr virus infection reveals an important role for early lytic viral protein expression in the development of lymphomas. *J Virol.* 2011;85(1):165-177.
11. Hong GK, Gulley ML, Feng WH, Delecluse HJ, Holley-Guthrie E, Kenney SC. Epstein-Barr virus lytic infection contributes to lymphoproliferative disease in a SCID mouse model. *J Virol.* 2005;79(22):13993-14003.
12. Long X, Li Y, Yang M, Huang L, Gong W, Kuang E. BZLF1 attenuates transmission of inflammatory paracrine senescence in Epstein-Barr virus-infected cells by downregulating tumor necrosis factor alpha. *J Virol.* 2016;90(17):7880-7893.
13. Kim JM, Chen DS. Immune escape to PD-L1/PD-1 blockade: seven steps to success (or failure) *Ann Oncol.* 2016;27(8):1492-1504.
14. Pham LV, Pogue E, Ford RJ. The Role of Macrophage/B-Cell Interactions in the Pathophysiology of B-Cell Lymphomas. *Front Oncol.* 2018;8:147.

FIGURE LEGENDS

Figure 1: Histological examination of the 2017 specimen. Effacement of the nodal architecture and cellular necrosis (Figure 1 A) with areas of grade 2 Follicular lymphoma (Figure 1B) intermingled with a diffuse proliferation of blastic elements (Figure 1C) were seen.

The neoplastic cells of the follicular component expressed BCL-2 (Figure 1D) as well as the diffuse component (Figure 1E). Fluorescent *in situ* hybridization (FISH) using break apart probes was positive for *BCL2* translocation both in the follicular and diffuse areas (inset 1D and 1E).

LMP-2A and EBV-encoded RNAs *in situ* hybridization positivity were present in scattered neoplastic cells within the follicles of the follicular areas (Figure 1F) and in 90% of the neoplastic cells in the diffuse areas (Figure 1G). Immunohistochemistry for ZEBRA was also positive in scattered larger cells in the diffuse areas (inset Figure 1G). A, original magnification (O.M.) 2,5 x; B-E, O.M. 10 x; F-G, O. M. 20x.

Figure 2: B-cell clonality , identical NTT and EBV positivity were demonstrated in all the specimens. Laser capture microdissection of the follicular and diffuse areas of the 2017 lymph node biopsy (Figure 2 A-B). A peak of 316 base pairs (bp) in length was identified both in follicular and diffuse components (Figure 2 C-D).

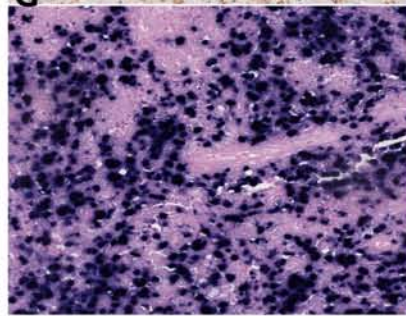
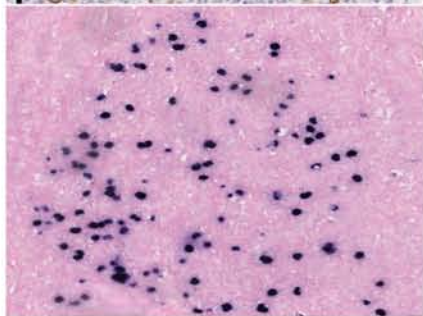
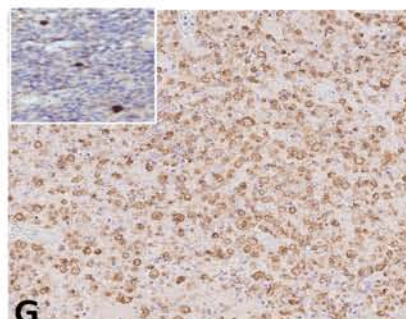
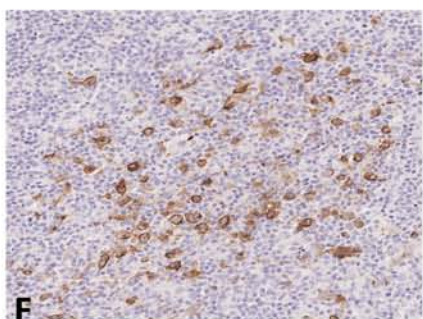
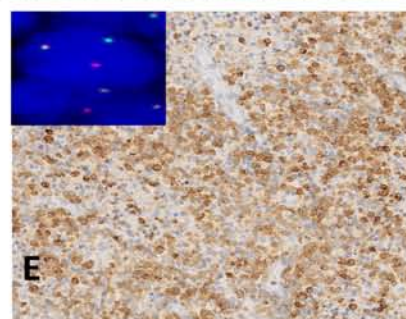
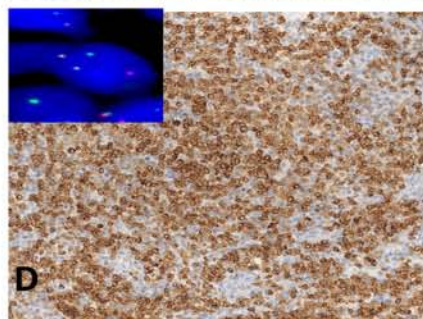
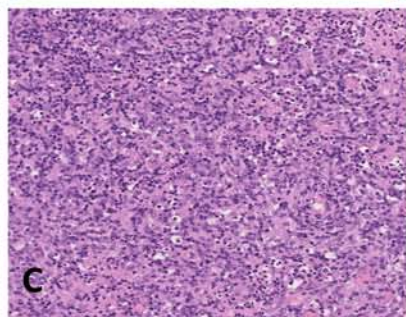
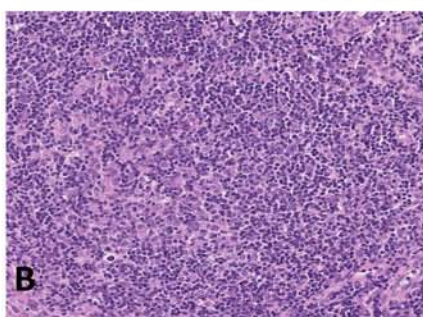
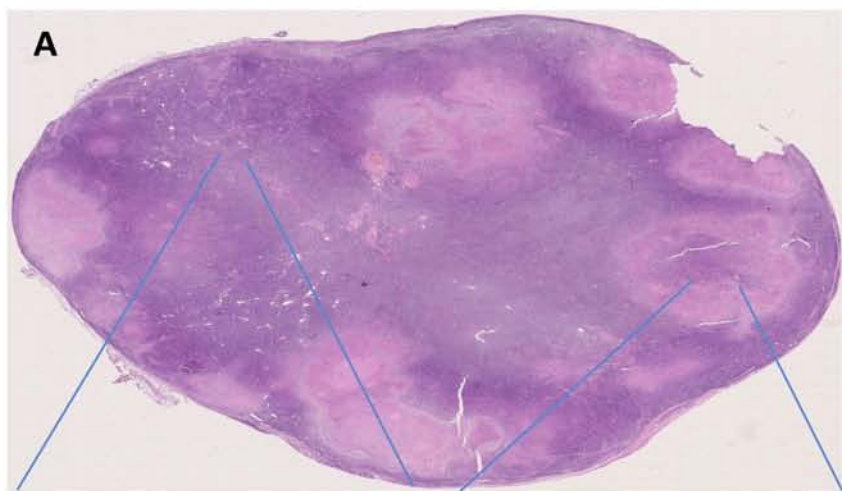
EBER *in situ* hybridization was positive in the 2011 and 2013 follicular lymphoma samples of the patient, increasing from the first (5%) to the second (10%) biopsy (Figure 2 E-F). The clonal analysis of the 2011 and 2013 FL samples identified a peak with the same length of the 2017 sample (316 bp) (Figure 2 G-H).

The corresponding FR1-JH PCR products of all the sample were directly sequenced and a productive IGHV-D-J rearrangement (V1-18*01, D3-9*01 and J4*02) with 86.76% omology of germ-line sequence was detected, confirming the clonal relationship (Figure 2 I).

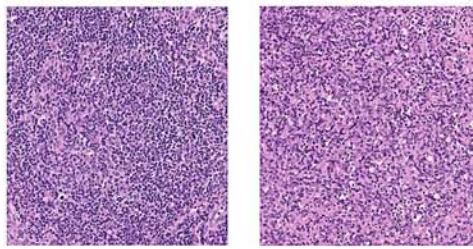
Furthermore, in all the biopsies, we detected an identical somatic hypermutation pattern and the same N-glycosylation motif (NTT) in the HCDR3 region, characteristic for FL (Figure 2 J). A-B, E-F original magnification 10x.

Figure 3: Time trend of the TME evolution. In the follicular lymphoma sample, the neoplastic follicles show a low number of regulatory T-cells (Figure 3 A-B) and exhausted T-cells (Figure 3 C). Numerous M2 macrophages were also found in the interfollicular areas accompanied by occasional M2 macrophages expressing PD-L1 (Figure 3 D).

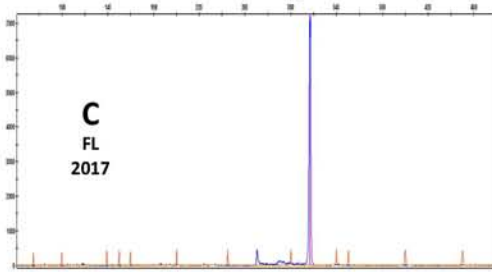
The diffuse large B cell lymphoma biopsy showed increased regulatory T-cells (Figure 3 E-F) and exhausted T-cells (Figure 3 G). The number of M2 macrophages was increased; the great majority of them expressed PDL-1 (Figure 3 H). PD-L1 expression was also demonstrated in scattered neoplastic cells by double staining with PAX-5 and PD-L1 (Figure 3 H inset). A-H, original magnification 20x.



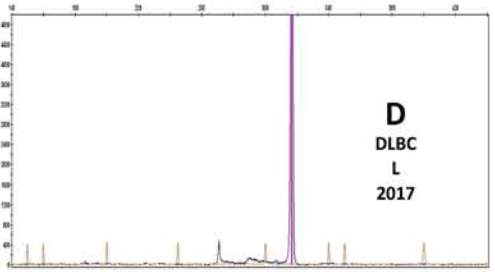
2017



A



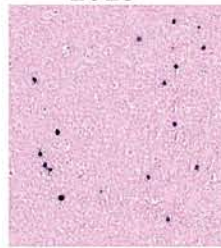
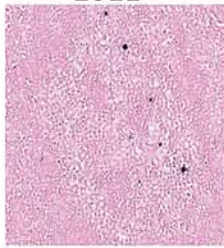
C
FL
2017



D
DLBC
L
2017

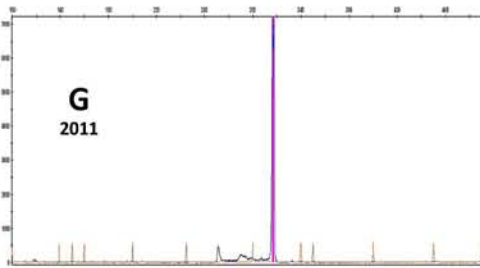
2011

2013

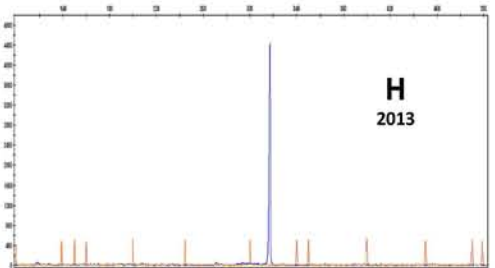


E

F

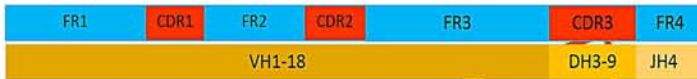


G
2011



H
2013

V-GENE and allele	V-DOMAIN Functionality	V-REGION identity % (nt)	J-GENE and allele	J-REGION identity % (nt)	D-GENE and allele	AA JUNCTION	JUNCTION frame
Homsap IGHV1-18*01 F	productive	86.76% (190/219 nt)	Homsap IGHJ4*02 F	83.87% (26/31 nt)	Homsap IGHDS-9*01 F	CALNTTGYFDYW	in-frame



J

Analysis of the JUNCTION

D-REGION is in reading frame 2.
Click on mutated (underlined) nucleotide to see the original one:

3'-V-REGION N1 D-REGION N2 5'-J-REGION J name D name
 tetgag... ctga ttattaccatgag..... g ..tacttgacatgtag Homsap_IGHJ4*02 Homsap_IGHV1-18*01

Translation of the JUNCTION

Click on mutated (underlined) amino acid to see the original one:

104 105 106 107 108 109 110 111 112 113 114 115 116 117 118 Frame CDR3- Junc length Molecular mass pI Physicochemical descriptor (by BRFAA)
 C Q I I V D V
 tpt ctc ctg tct tca gaa tcc cgg tac ctg gac txc tgg + 11 1,554.7 3.75 CALNTTGYFDYW

NTT

N-Glycosilation SiteNXS/T Asparagina-X-Serina/Treonina

